Prediction of the Nominal Bending Moment Capacity for Plain and Singly Reinforced Rectangular RPC Beam Sections

Dr. Hisham M. Al-Hassani
Building and Construction Engineering Department, University of Technology/ Baghdad
Dr. Wasan I. Khalil
Building and Construction Engineering Department, University of Technology/ Baghdad
Email: wasan1959@yahoo.com
Lubna S. Danha
Building and Construction Engineering Department, University of Technology/ Baghdad

Received on:15/10/2014 & Accepted on:7/5/2015

ABSETRACT

A new generation of Ultra High Performance Concrete (UHPC) named Reactive Powder Concrete (RPC) was developed in the last decades, which offers, superior strength, durability and ductility. One of the main differences between other concretes and RPC is that the latter requires mechanical models capable of taking tensile behavior into account for structural application to enable the material to be fully exploited. The complete stress-strain relationship under direct tensile test and uniaxial compression of different RPC mixes was experimentally investigated. Nonlinear equations are suggested to model the complete tensile and compressive stress-strain relationship for all the RPC mixes studied. In this research an analytical study is devoted to establish a simple equation for predicting the nominal bending moment capacity M_n of plain and singly reinforced rectangular RPC beam sections. The equation derived showed good agreement with all the flexural test results performed in previous researches and some other investigations on reactive powder concrete beams.

Keywords: Reactive Powder Concrete, Stress-Strain Relationship, Singly Reinforced RPC Beams.

تقدير عزم الانحناء الاسمي الاقصى لعتبات خرسانة المساحيق الفعالة بمقاطع مستطيلة غير مسلحة ومفردة التسليح

الخلاصة

يعتبر الجيل الجديد من الخرسانة فائقة الاداء والمسمى بخرسانة المساحيق الفعالة والذي تم تطويره في العقود الاخيرة ذو ميزات عديدة فهو يوفر مقاومة وديمومة ومطيلية متفوقة. ان أحد الاختلافات الرئيسية بين انواع الخرسانة الاخرى وخرسانة المساحيق الفعالة هو ان النوع الاخير يحتاج الى موديلات ميكانيكية قادرة على أخذ سلوك الشد في الاعتبار لإمكانية استغلال المادة بشكل كامل في التطبيقات الانشائية. تم ايجاد العلاقة المتكاملة للإجهاد- الإنفعال في حالتي الشد المحوري والانضغاط المحوري لخرسانة المساحيق الفعالة مختبرياً. أقترحت معادلات لا خطية لتمثيل العلاقة المتكاملة للإجهاد- الإنفعال في حالتي الشد المحوري والانضغاط المحوري لخرسانة المساحيق الفعالة. يتضمن هذا البحث ايجاد معادلة بسيطة لتخمين عزم الانحناء الاسمي الاقصى لمقاطع مستطيلة غير مسلحة ومفردة التسليح من عتبات خرسانة المساحيق الفعالة. أظهرت المعادلة المشتقة توافقاً جيداً مع نتائج فحص الانحناء التي أجريت في بحوث مختبرية السابقة وبعض البحوث السابقة الأخرى على عتبات خرسانة المساحيق الفعالة.

INTRODUCTION

Structural designers continually seek new approaches and ideas that will make their structures more aesthetically pleasing, functionally effective, and cost efficient. Historically, the improvement of structures depends strongly upon the characteristics of engineering materials. A new kind of material with excellent properties usually results in a revolution in structures **[1]** Recently a new generation of Ultra High Performance Concrete (UHPC) named Reactive Powder Concrete (RPC) has been developed, that offers superior strength, durability and ductility. The superior strength of RPC leads to more slender structures resulting in a significant dead load reduction**[2]**. The superior tensile strength of RPC is such that the concrete itself can carry all but the primary tensile stresses. The elimination of shear and other auxiliary reinforcing steel allows nearly limitless freedom of shape for structural members and major cost savings can be realized **[2]**. RPC provides improved seismic performance by reduction of inertia loads with lighter members, allowing large deflections with reduced cross sections, and providing higher energy absorption**[3]**. RPC has a high resistance to abrasive wear, which is ideal in applications where physical wear greatly limits the life of more conventional concrete, i.e. bridge decks and industrial floors **[2]**. Also RPC has superior corrosion resistance provides protection from chemicals and continuous exposition to humidity **[4]**.

UHPC are particularly suitable for precast structures, but their use on site is possible and can be completely relevant. The preferred areas of applications may include structures or part of structures subjected to aggressive environments, structures under shocks effects and composite structures **[5].** UHPC properties make it a viable material for thin-bonded concrete bridge deck overlays **[6]** and for rehabilitation of old bridge **[7]**. UHPC used in many architectural applications **[8, 9, 10]**.

Voo et al. [11] examined many specimens of RPC for the two point flexural tensile strength. They used two types of steel fibers with 2.5% volume fraction, straight fibers with aspect ratio of 65 and end hooked fibers with aspect ratio of 60. The results shows that end hooked fibers perform better than straight fibers. The results indicated an

increase in flexural strength by more than 8% for end hooked fibers compared to straight fibers. **Yang et al. [12]** examined the flexural behavior of UHPC beams (180×270×2900 mm) with steel rebar ratios less than 0.02 (0.006, 0.009, 0.012, 0.0131, 0.0196) and straight steel fibers with a volumetric ratio of 2% and aspect ratio of 65. The UHPC was placed using two methods (placing UHPC in one end of the form and allowed to flow to the other end to complete the filling process or placing UHPC in midspan and allowed to flow to both ends of the form). It was observed that placing the UHPC at the end of the beam provides better structural performance than placing the UHPC at midspan. Steel fiber reinforced UHPC exhibited effective ductile behavior due to the yielding of the rebar until flexural failure for the UHPC beam with low rebar ratios.

There is very limited number of researches on tensile behavior (tensile stress-strain response, strain hardening) of RPC. In previous studies [13, 14] the tensile behavior of RPC as well as some mechanical properties of RPC composite with the effect of three variables (steel fibers volumetric ratio, silica fume content and superplasticizer type) was studied. The complete tensile stress-strain relationship under direct tensile test and compressive stress-strain relationship under uniaxial compression of different RPC mixes was experimentally investigated. Nonlinear equations are suggested to model the complete tensile stress-strain relationship and the complete compressive stress-strain relationship for all the RPC mixes studied. In this research an analytical study is devoted to establish a simple equation for predicting the nominal bending moment capacity M_n of singly reinforced rectangular RPC sections. The proposed M_n equation is derived based on equivalent stress blocks for both compression and tension.

Design Stress Block Of Rpc Section

The actual bending stress distribution across the depth of RPC section subjected to pure bending moment can be converted into a simple equivalent stress distribution which is accurate enough to be used in analysis and design. Fig.(1) shows a typical stress-strain curve of RPC in compression. This curve is representative of the experimental curves obtained for different RPC mixes in previous research [14]. In order to make use of this f_c – ε_c relationship in the design and analysis of flexural RPC members, it is proposed in this research to simplify such behavior and convert it into an equivalent bi-linear relationship which is plotted as dashed line in the same Fig. (1). This dashed line consists of an ascending straight line (from zero stress to the 0.9 f'_c) and a constant stress line (at stress level equal to 0.9 f'_c). The adopted dashed line is terminated at a value of maximum strain equals 1.5 ε_o (where ε_o is the strain corresponding to the peak stress f'_c). It is proposed that this maximum strain value can be considered as the ultimate compressive strain of RPC (εcu) such that;

$$\varepsilon_{cu} = 1.5\ \varepsilon_o$$

It is important to note that the proposed equivalent compressive stress-strain relationship of RPC is based on the following two facts;

1- The equivalent area under the dashed line is nearly equal to the area under the actual curve.

2- The centriod of the equivalent area is very close to the centriod of the actual area.

In that previous research [14], many typical stress-strain curves of different RPC mixes in tension were obtained from experimental work. According to these curves, the tensile stress-strain curve with strain hardening behavior given by Fig. (2) is adopted in this investigation to represent the stress-strain curve of RPC in tension. In order to make use of this $f_t - \varepsilon_t$ relationship in the design and analysis of flexural RPC members, it is proposed in present research to simplify such behavior and convert it into an equivalent elastic perfectly plastic response. This is represented by the dashed line (idealized line) shown in Fig.(2) with the elastic response of this idealization terminating at the point whose strain-stress coordinates are (ε_{te} , f_{te}), which represent concrete first cracking tensile strain and strength respectively.

Basic Conditions

The analysis of RPC rectangular section will be carried out based on the following assumptions;

1- The RPC rectangular section to be analyzed under pure bending moment is under-reinforced such that at ultimate stage it fails according to the tensile type of failure.
2- The strain distribution across the depth of the RPC section is linear
3- Perfect bond exists between concrete composite and longitudinal steel reinforcement. This means that the strains in the longitudinal steel and concrete at the same level are equal and no slippage failure of steel reinforcement can occur.
4- Strain hardening of steel bars is neglected.
5- The compression zone is defined by an equivalent bi-linear stress block.
6- Strain hardening behavior is adopted to represent the stress-strain curve of RPC in tension.
7- The tension zone is defined by an equivalent bi-linear stress block.

Analysis of Rpc Section Under Pure Bending

Design codes always adopt design equations that have two characteristics, first they must be safe in estimating the member cross section capacity, and secondly they must be as simple as possible so that they can be applied with minimum effort and time.

According to Codes of Practice, reinforced concrete sections must be flexurally designed as under-reinforced so that at failure the longitudinal steel bars yield before the concrete in the compression zone can crush, giving an important required warning.

Fig. (3) shows a rectangular RPC section of a width b and total depth h, reinforced in the tension zone with steel bars of area A_s located at an effective depth d. The section is subjected to a positive bending moment M such that at ultimate stage the strain and actual stress distributions are as shown in the same figure. The figure also shows a conversion of the actual stress blocks to equivalent bi-linear stress blocks for both compression and tension as proposed in this research.

Referring to the strain and equivalent stress distributions of Fig.(3), from strain compatibility:

$$\frac{x_{c1}}{\varepsilon_{c1}} = \frac{c}{\varepsilon_{cu}}$$

$$\therefore \quad x_{c1} = \frac{\varepsilon_{c1}}{\varepsilon_{cu}}\, c \qquad \cdots\cdots (1)$$

$$\frac{x_{t1}}{\varepsilon_{te}} = \frac{c}{\varepsilon_{cu}}$$

$$\therefore \quad x_{t1} = \frac{\varepsilon_{te}}{\varepsilon_{cu}}\, c \qquad \cdots\cdots (2)$$

where:

$$\varepsilon_{c1} = \frac{0.9 f'_c}{Ec} \qquad \cdots\cdots (3)$$

$$\varepsilon_{cu} = 1.5\, \varepsilon_o \qquad \cdots\cdots (4)$$

Depending on the equivalent stress distribution shown in Fig.(3), the values of the compressive forces $\boldsymbol{C_1}$ and $\boldsymbol{C_2}$ and the tensile forces $\boldsymbol{T_{c1}}$, $\boldsymbol{T_{c2}}$ and $\boldsymbol{T_S}$ are listed below;

$$C_1 = 0.45\, f'_c\, b\, x_{c1} \qquad \cdots\cdots (5)$$
$$C_2 = 0.9\, f'_c\, b\, (c - x_{c1}) \qquad \cdots\cdots (6)$$
$$T_{c1} = 0.5\, f_{te}\, b\, x_{t1} \qquad \cdots\cdots (7)$$
$$T_{c2} = f_{te}\, b\, (h - c - x_{t1}) \qquad \cdots\cdots (8)$$
$$T_s = A_s\, f_y \qquad \cdots\cdots (9)$$

The locations of such forces from the neutral axis are listed below;

For C_1 ; $Y_{c1} = \frac{2}{3}\, x_{c1}$ ..... (10)

For C_2 ; $Y_{c2} = \frac{1}{2}\, (c + x_{c1})$ ..... (11)

For T_{c1} ; $Y_{tc1} = \frac{2}{3}\, x_{t1}$ ..... (12)

For T_{c2} ; $Y_{tc2} = \frac{1}{2}\, (h - c + x_{t1})$ ..... (13)

For T_s ;

$Y_{ts} = d - c$ .. .... (14)

The total compressive force on the RPC section can therefore be calculated as;

$$\boldsymbol{C} = C_1 + C_2$$
$$= f'_c\, b\, (0.9\, c - 0.45\, x_{c1})$$
$$= \frac{f'_c\, b\, c}{\varepsilon_{cu}} (0.9\, \varepsilon_{cu} - 0.45\, \varepsilon_{c1}) \qquad \cdots\cdots (15)$$

while the total tensile force on the RPC section can be calculated as;

$$T = T_{c1} + T_{c2} + T_s$$
$$= f_{te}\, b\, (h - c - 0.5\, x_{t1}) + A_s f_y$$
$$= f_{te}\, b\, h - \frac{f_{te}\, b\, c}{\varepsilon_{cu}} (\varepsilon_{cu} + 0.5\, \varepsilon_{te}) + A_s f_y \qquad \ldots\ldots (16)$$

From equilibrium;

$$C = T$$

$$\frac{f'_c\, bc}{\varepsilon_{cu}}(0.9\varepsilon_{cu} - 0.45\,\varepsilon_{c1}) = f_{te}\, bh - \frac{f_{te}\, bc}{\varepsilon_{cu}}(\varepsilon_{cu} + 0.5\varepsilon_{te}) + A_s f_y$$

$$c = \frac{\left(f_{te}\, b\, h + A_s f_y\right)\varepsilon_{cu}}{f'_c\, b\,(0.9\,\varepsilon_{cu} - 0.45\,\varepsilon_{c1}) + f_{te}\, b\,(\varepsilon_{cu} + 0.5\,\varepsilon_{te})} \quad \ldots\ldots(17)$$

Eq. (17) gives the location of neutral axis measured from top compression fiber.
The nominal ultimate bending moment capacity of a singly reinforced rectangular RPC section can be determined by summing up the moments around the neutral axis caused by all the compressive and tensile forces on the section such that;

$$M_n = M_{c1} + M_{c2} + M_{tc1} + M_{tc2} + M_s$$

$$M_n = 0.45 f'_c\, b\left(c^2 - \frac{x_{c1}{}^2}{3}\right) + 0.5 f_{te}\, b\left(h^2 + c^2 - 2hc - \frac{x_{t1}{}^2}{3}\right) + A_s f_y(d - c) \quad \ldots(18)$$

Evaluation of The Proposed Moment Capacity Equation
Comparison with Experimental Results

The accuracy of Equation (18) can be examined through comparison with the results of (47) experimental tests. Ten of these tests were performed in previous investigation on plain RPC beams [14], while the other 37 tests were conducted by other investigators [11,15,12,16] on plain and singly reinforced RPC beams. The data used represents a wide range of RPC cylinder compressive strength (83-197) MPa and different types of steel fibers (straight and hooked) with volume fractions ranging between (0% - 3%). Table (1) shows the complete details of these (47) beams and the results of calculations. Eq. (18) gives a mean value (μ) of $M_{n\ predicted}$ / $M_{n\ exp.}$ (for the 47 beams used in this comparison) of 0.91 with standard deviation (SD) of 0.105 and coefficient of variation (COV) of 11.52%. Fig. (4) shows the ratio $M_{n\ predicted}$ / $M_{n\ exp.}$ versus the cylinder compressive strength f'_c [13], while Fig. (5) shows the nominal ultimate bending moment capacity obtained from the experimental work versus the corresponding theoretical value from Eq. (18) (predicted).

Figs. (4) and (5) together with Table (1) reveal that M_n predicted by the proposed equation (18) is slightly less than M_n observed experimentally for the majority of the beams tested in previous researchs [13, 14]and by other investigators [11,15,12,16]. Therefore Eq. (18) is a conservative equation and can safely be used in design and analysis after multiplied by a certain reduction factor to be specified by codes of practice. However, it is only for beams No. (7, 8, 35, 40, and 44) as given in Table (1) that Eq. (18) gives overestimated values in comparison with the corresponding experimental values. This can be attributed to the type of failure of these beams. The tensile stress-strain response of the nonfibrous RPC specimens and specimens with steel fibers volume fraction of 1% failed immediately after crack initiation exhibiting a strain softening tensile stress-strain behavior [14]. Beams No. (7, 8, 35, 40, and 44) having steel fibers volume fraction of (0, 1, 1, 1.25, and 1) respectively might be shown such behavior. However, the derivation of Eq. (18) for M_n is based on considering a strain hardening

type of tensile behavior; this explains why Eq. (18) gives a higher value than the corresponding experimental value for beams No. (7, 8, 35, 40, and 44).

It can be concluded from the comparison with the experimental results that the proposed M_n equation (18) is a reliable equation and can be used safely to get accurate estimates of nominal moment capacity for plain and singly reinforced rectangular RPC sections subjected to pure bending moment. Therefore to use this equation in analysis and design, the following properties must be specified first;

§ The dimension of the beam cross section (**b** and **h**).

§ The steel bar properties [yield stress, area of longitudinal steel bars, effective depth of longitudinal steel bars (f_y, A_s, and d respectively)].

§ The RPC properties [cylinder compressive strength of concrete and volume fraction of fiber (f'_c and V_f % respectively)].

while the other RPC properties including, first cracking tensile strength, modulus of elasticity, compressive strain corresponding to f'_c, first cracking tensile strain(f_{te} , Ec, ε_o ,and ε_{te} respectively**)** can directly be determined from the following Equations [14]:

$$f_{te} = 0.0243(f'_c) + 1.848(V_f) \quad \text{…….. (19)}$$

$$Ec = 113.43(f'_c) + 31126.74 \quad \text{…….. (20)}$$

$$\varepsilon_o = 1.17\times10^{-5}(f'_c) + 4.59\times10^{-4}(V_f) + 1.92\times10^{-3} \quad \text{…….. (21)}$$

$$\varepsilon_{te} = 2.17*10^{-5}(f_{te}) + 1.75*10^{-5} \quad \text{..…….. (22)}$$

Comparison with Similar Existing Theoretical Equations

The suggested moment capacity equation (18) can also be compared with similar theoretical equations derived separately by **Hannawayya** [15] and **Al-Hassani and Ibraheem** [17] to determine the nominal ultimate bending moment capacity of singly reinforced rectangular RPC sections. **Hannawayya** [15] derived two equations to predict M_n; one based on actual stress and strain distributions on the section as shown in Fig. (6), while the other equation was derived based on the simplified stress and strain distributions given by **ACI committee 544** [18] for fibrous concrete as shown in Fig. (7). In both solutions, horizontal equilibrium of compressive and tensile forces on the RPC section was considered and the sum of the moments of these internal forces about the neutral axis gave the desired M_n equation. Thus;

1. By following the strain and stress distribution of Fig. (6);

$$M_n = \left[b\left(\alpha\frac{x1^5}{5} + \beta\frac{x1^4}{4} + \gamma\frac{x1^3}{3}\right) + bf'_c\left(\frac{c^2 - x1^2}{2} - \frac{0.15}{\varepsilon_{cu} - \varepsilon_o}\left(\frac{c^3 - x1^3}{3c}\varepsilon_{ef}\frac{c^2 - x1^2}{2}\varepsilon_0\right)\right)\right]$$
$$+ \left[\frac{bf_r c^2}{6}\left(\frac{\varepsilon_{cr}}{\varepsilon_{ef}}\right)^2\left(2 + 3\lambda\left(\left(\frac{h}{c} - 1\right)^2\left(\frac{\varepsilon_{ef}}{\varepsilon_{cr}}\right)^2 - 1\right)\right)\right]$$
$$+ \left[\left(f_y + H(\varepsilon_s - \varepsilon_y)\right)A_s(d - c)\right] \quad \text{..(23)}$$

where:

$$\alpha = A \left(\frac{\varepsilon_{ef}}{c}\right)^3 f'_c$$
$$\beta = B \left(\frac{\varepsilon_{ef}}{c}\right)^2 f'_c$$
$$\gamma = C \left(\frac{\varepsilon_{ef}}{c}\right) f'_c$$

It can be seen that Eq. (23) is very complicated and requires much time and effort to solve as compared to the suggested equation (18) of the present work. The values of the constants A, B, and C in equation (23) depend on the compressive stress-strain relationship obtained by **Hannawayya** [15] which was different from one RPC mix to another. Therefore Eq. (23) cannot be applied to the beams conducted by other investigators.

2. By following the strain and simplified stress distributions of Fig. (7);

$$M_n = \gamma_1 f'_c \beta_1 c^2 b \left(1 - \frac{\beta_1}{2}\right) + f_y A_s (d - c) + \frac{f_r b}{2} \left((h-c)^2 - x_e{}^2 \right) \quad \ldots (24)$$

where:

$$\mathbf{x_e} = \sqrt{\frac{(\mathbf{h}-\mathbf{c})^2(\mathbf{1}-\boldsymbol{\lambda})}{\mathbf{d^2}} + \frac{\mathbf{x_{cr}}^2 \left(\boldsymbol{\lambda} - {}^{\mathbf{2}}/_{\mathbf{3}}\right)}{\mathbf{d^2}}}\ \mathbf{d}$$

$$\boldsymbol{\gamma_1} = \mathbf{1} - \frac{\mathbf{1.71}}{\mathbf{100}} \left(\boldsymbol{f'_c V_f}\right)^{\mathbf{2.85}}$$

$$\boldsymbol{\beta_1} = \mathbf{0.922} - \frac{\mathbf{1.92}}{\mathbf{100}} \left(\boldsymbol{f'_c V_f}\right)^{\mathbf{3.23}}$$

$$\boldsymbol{x_{cr}} = \frac{\boldsymbol{\varepsilon_{cr}}}{\boldsymbol{\varepsilon_{ef}}} \boldsymbol{c}$$

$\boldsymbol{\lambda}$ = post cracking tensile stress factor whose value (usually ranges between zero and 0.99) depends mainly on the steel fibers ratio, existence of steel bar reinforcement, strength of the matrix and partially on longitudinal steel reinforcement ratio.

Hannawayya [15] limited his solution of $\boldsymbol{M_n}$ (Eq. 24) to RPC having cylinder compressive strength ranging between (79-110) MPa and steel fibers ratio ranging between (0%−2%). Applications of Eq. (24) outside these ranges can give unreasonable value of γ1 and β1. For instance the application of Eq. (24) to beams No. 11-22 [given in Table (1)] gave negative values for β1. Nevertheless, Fig. (8) shows a comparison between the wide spectrum values of $\boldsymbol{M_n}$ calculated by Eq. (18) of the present research and the limited values of $\boldsymbol{M_n}$ given by **Hannawayya [15]**(Eq. 24).

Al-Hassani and Ibraheem [17] derived an equation for determining the nominal ultimate bending moment capacity $\boldsymbol{M_n}$ of singly reinforced rectangular RPC sections based on the strain and equivalent stress distributions shown in Fig. (9). Horizontal equilibrium of compressive and tensile forces on the RPC section was considered and the moments of these internal forces about the neutral axis were summed up to give;

$$\boldsymbol{M_n} = \frac{\mathbf{1}}{\mathbf{4}} \left(\frac{\mathbf{5}}{\mathbf{6}}\ \boldsymbol{\alpha} + \mathbf{1}\right) \left(\frac{\boldsymbol{c}}{\boldsymbol{d}}\right)^2 \boldsymbol{f'_c}\, \boldsymbol{b}\, \boldsymbol{d^2} + \boldsymbol{A_s}\, \boldsymbol{f_y}\, \boldsymbol{d} \left(\mathbf{1} - \frac{\boldsymbol{c}}{\boldsymbol{d}}\right)$$

$$+\left[\frac{1}{2}\left(\frac{h}{d}\right)^2-\left(\frac{h}{d}\right).\left(\frac{c}{d}\right)+\frac{1}{2}\left(1-\frac{{\varepsilon_t}^2}{4{\varepsilon_0}^2}\right)\left(\frac{c}{d}\right)^2\right] f_t\, b\, d^2 \quad \ldots(25)$$

where:

$$\frac{c}{d}=\frac{\left[\rho\frac{f_y}{f'_c}+\frac{f_y}{f'_c}\left(\frac{h}{d}\right)\right]}{\left[\frac{f_t}{f'_c}\left(1+\frac{\varepsilon_t}{2\varepsilon_o}\right)+\frac{1}{2}\left(1+\frac{\alpha}{2}\right)\right]}$$

$$\frac{\varepsilon_t}{\varepsilon_o}=0.1$$

$$\alpha=\frac{stress\ corresponding\ to\ strain\ 2\varepsilon_o}{f'_c}$$

It can be seen that Eq. (25) is not simple to use and requires much time and effort to solve as compared to the suggested equation (18) of the present work. Fig. (10) shows that some of the M_n values predicted by **Al-Hassani and Ibraheem** [17] are overestimated in comparison with the corresponding experimental values. Therefore their equation (25) must be multiplied by a higher reduction factor if used in design and analysis to ensure safe predictions of nominal ultimate bending moment capacity.

Conclusions

The equation derived to predict the nominal ultimate bending moment capacity (M_n) of plain and singly reinforced rectangular RPC sections (based on idealized compressive and tensile stress blocks) showed good agreement with all the flexural test results performed previous researches and some other investigations. So it can be used safely and with good accuracy in the analysis and design of RPC beams having cylinder compressive strength within the range 83-197 MPa and steel fibers ratio within the range 0% - 3%.

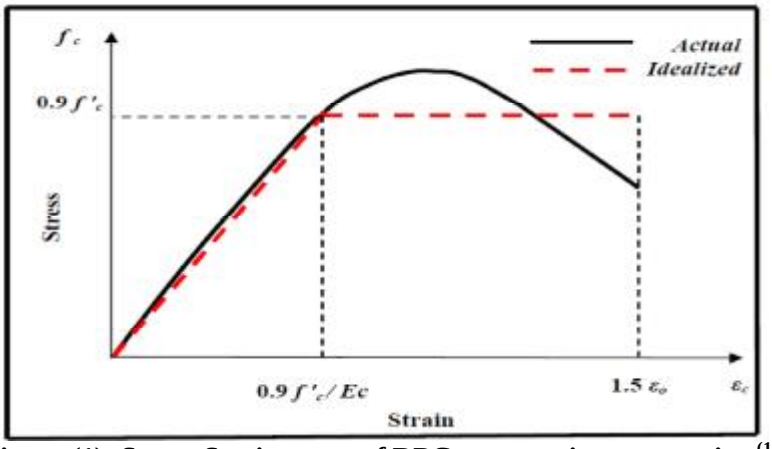

Figure (1): Stress-Strain curve of RPC concrete in compression [14]

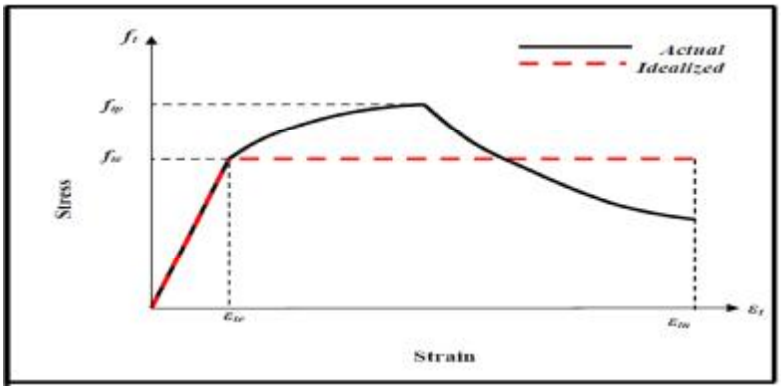

Figure (2): Actual and idealized stress-strain curve of RPC in tension [14]

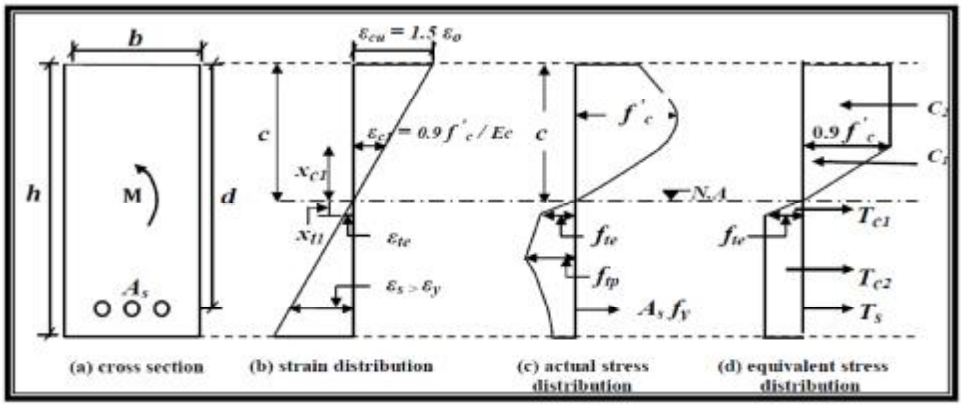

Figure (3): Actual and proposed equivalent stress distributions at ultimate stage through a singly reinforced rectangular RPC section subjected to pure bending moment

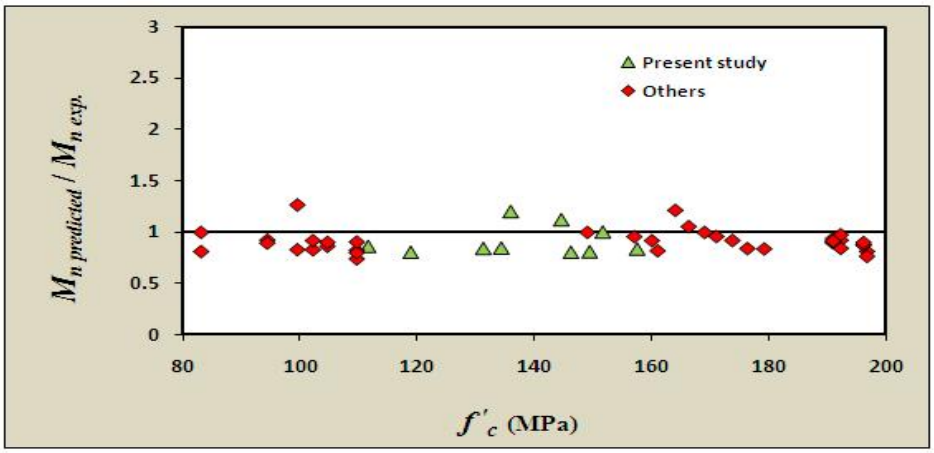

Figure (4): The ratio $M_{n\ predicted} / M_{n\ exp.}$ versus the cylinder compressive strength f'_c

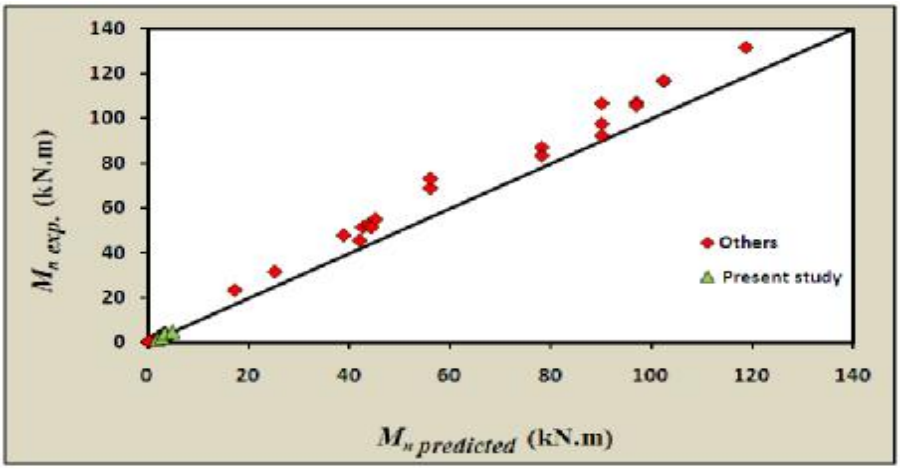

Figure (5): Experimental versus predicted values of the nominal bending moment capacity

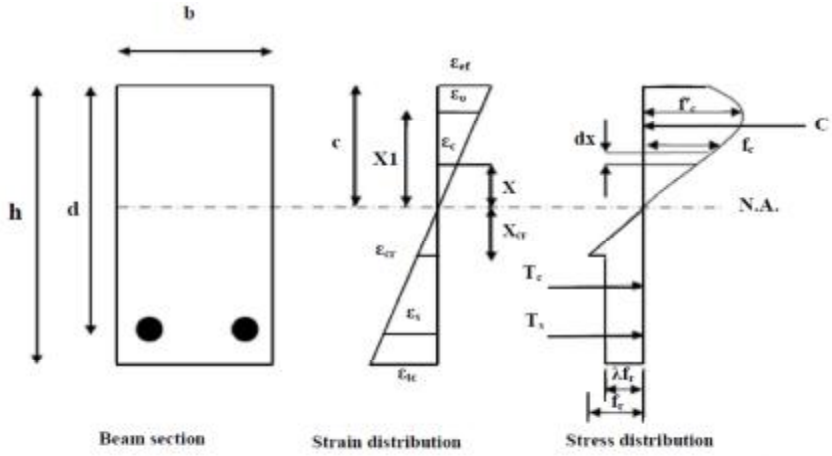

Figure(6) Strain and stress distribution through RPC beam cross section adopted by Hannawayya [15]

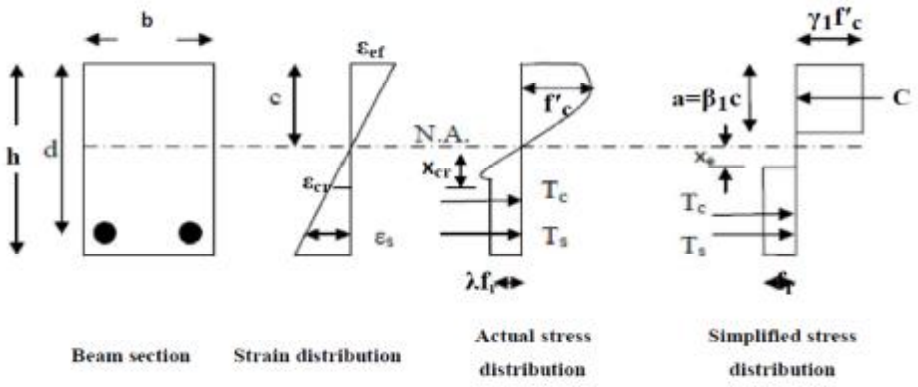

Figure (7) Simplified design model for analysis of singly reinforced RPC section adopted by Hannawayya [15]

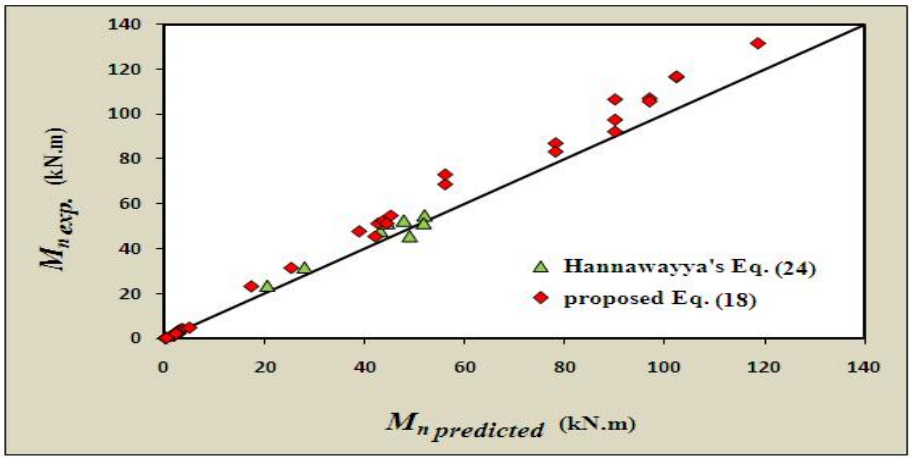

Figure (8): Comparison between M_n values predicted by Hannawayya [15] and the experimental research [14]

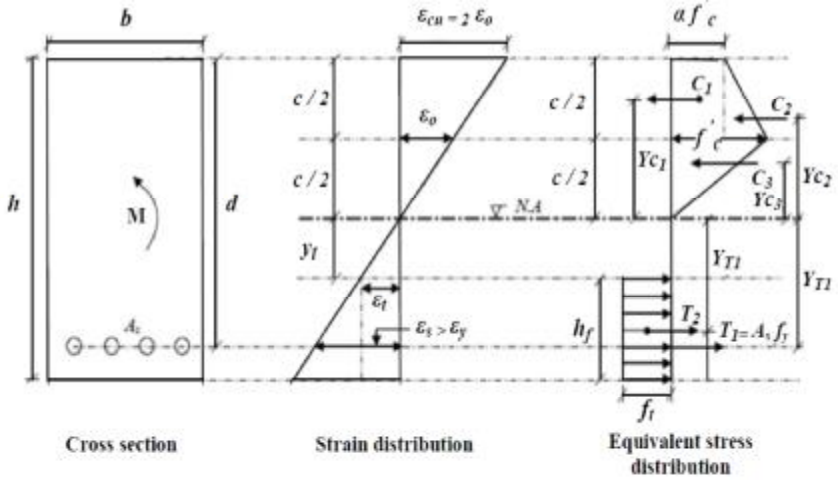

Figure (9) Strain and stress distributions through RPC beam cross section adopted by Al-Hassani and Ibraheem [17]

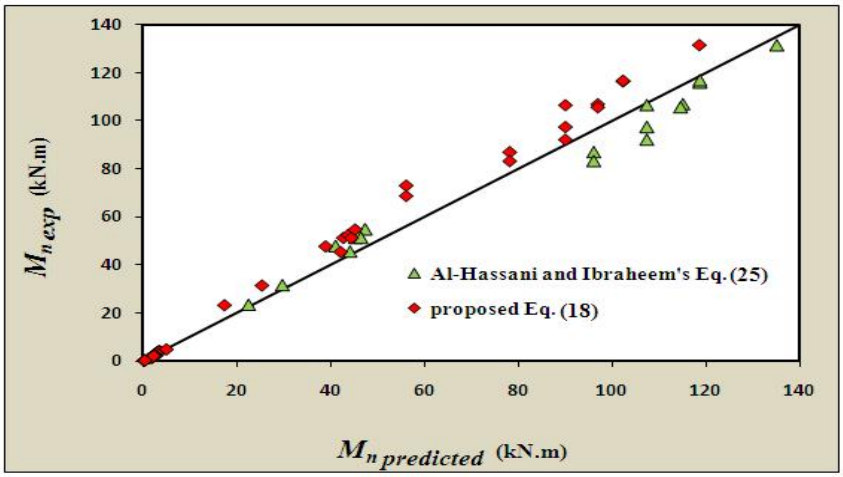

Figure (10): Comparison between M_n values predicted by Al-Hassani and Ibraheem[17] and the experimental research[14]

Table (1): Comparison between predicted and experimentalnominal bending moment from many researches

No.	V_f %	fiber type*	lf/df	ρ	d (mm)	b (mm)	h (mm)	f_y (MPa)	f'_c (MPa)	ε_o $\times 10^{-3}$	Ec (GPa)	f_{te} (MPa)	ε_{te} $\times 10^{-4}$	M_n predicted Eq. (5-18) (kN.m)	$M_{n\,exp.}$ (kN.m)	$\frac{M_{n\,pred.}}{M_{n\,exp.}}$	Reference
1	2	H	60	0	0	100	100	0	118.91	4.12	44.841	6.17	1.54	2.8	3.5	0.80	Present study and previous research (14)
2	2	H	60	0	0	100	100	0	134.33	4.36	46.398	6.74	1.64	3.2	3.8	0.84	
3	2	H	60	0	0	100	100	0	111.66	4.18	43.836	6.47	1.70	3.0	3.5	0.86	
4	2	H	60	0	0	100	100	0	131.27	4.46	45.900	6.59	1.69	3.1	3.7	0.84	
5	2	H	60	0	0	100	100	0	146.19	4.84	47.422	6.68	1.68	3.2	4.0	0.80	
6	2	H	60	0	0	100	100	0	157.48	4.63	49.103	7.32	1.61	3.5	4.2	0.83	
7	0	-	-	0	0	100	100	0	135.93	3.52	46.262	3.64	0.90	1.8	1.5	1.20	
8	1	H	60	0	0	100	100	0	144.57	3.95	47.363	5.80	1.41	2.8	2.5	1.12	
9	2	H	60	0	0	100	100	0	149.39	4.59	48.295	6.78	1.62	3.3	4.1	0.80	
10	3	H	60	0	0	100	100	0	151.62	4.97	48.538	10.51	2.45	4.9	4.9	1.00	
No.	V_f %	fiber type*	lf/df	ρ	d (mm)	b (mm)	h (mm)	f_y (MPa)	f'_c (MPa)	ε_o^{++} $\times 10^{-3}$	Ec (GPa)	f_{te}^{+++} (MPa)	ε_{te}^{++++} $\times 10^{-4}$	M_n predicted Eq. (5-18) (kN.m)	$M_{n\,exp.}$ (kN.m)	$\frac{M_{n\,pred.}}{M_{n\,exp.}}$	Reference
11	2	S	65	0	0	180	270	0	196.7	5	46.818	9	2.13	56.1	68.8	0.82	Yang et al. (12)
12	2	S	65	0	0	180	270	0	196.7	5	46.818	9	2.13	56.1	73.1	0.77	
13	2	S	65	0.006	235	180	270	420	190.9	4.94	46.418	8.81	2.09	78.2	87	0.90	
14	2	S	65	0.006	235	180	270	420	190.9	4.94	46.418	8.81	2.09	78.2	83.3	0.94	

Table (1) – continued.

No.	V_f %	fiber type*	lf/df	ρ	d (mm)	b (mm)	h (mm)	f_y (MPa)	f'_c (MPa)	ε_o ** $\times 10^{-3}$	Ec (GPa)	f_{te} *** (MPa)	ε_{te} **** $\times 10^{-4}$	M_n predicted Eq. (5-18) (kN.m)	$M_{n\,exp.}$ (kN.m)	$\frac{M_{n\,pred.}}{M_{n\,exp.}}$	Reference
15	2	S	65	0.009	235	180	270	420	192.2	4.95	46.680	8.85	2.10	90.1	97.5	0.92	Yang et al. (12)
16	2	S	65	0.009	235	180	270	420	192.2	4.95	46.680	8.85	2.10	90.1	106.6	0.85	
17	2	S	65	0.009	235	180	270	420	192.2	4.95	46.680	8.85	2.10	90.1	92.2	0.98	
18	2	S	65	0.012	235	180	270	420	196.1	4.99	45.530	8.98	2.12	102.4	116.5	0.88	
19	2	S	65	0.012	235	180	270	420	196.1	4.99	45.530	8.98	2.12	102.4	116.8	0.88	
20	2	S	65	0.0131	215	180	270	420	190.9	4.94	46.418	8.81	2.09	97.0	107	0.91	
21	2	S	65	0.0131	215	180	270	420	190.9	4.94	46.418	8.81	2.09	97.0	105.7	0.92	
22	2	S	65	0.0196	215	180	270	420	196.1	4.99	45.530	8.98	2.12	118.7	131.6	0.90	
No.	V_f %	fiber type*	lf/df	ρ	d (mm)	b (mm)	h (mm)	f_y (MPa)	f'_c (MPa)	ε_o $\times 10^{-3}$	Ec (GPa)	f_{te} *** (MPa)	ε_{te} **** $\times 10^{-4}$	M_n predicted Eq. (5-18) (kN.m)	$M_{n\,exp.}$ (kN.m)	$\frac{M_{n\,pred.}}{M_{n\,exp.}}$	Reference
23	0.5	S	65	0.0819	97.5	125	140	570	83.109	3.6	52.885	2.38	0.69	38.9	47.8	0.81	Hannawayya (05)
24	1	S	65	0.0819	97.5	125	140	570	99.527	4.4	50.379	3.86	1.01	42.7	51.3	0.83	
25	1.5	S	65	0.0819	97.5	125	140	570	102.20	4.8	58.265	4.88	1.23	43.7	52.5	0.83	
26	2	S	65	0.0819	97.5	125	140	570	109.65	4.9	38.432	6.06	1.49	45.2	54.8	0.82	
27	2	S	65	0.0819	97.5	125	140	570	104.66	4.4	46.171	5.89	1.45	44.4	51.3	0.87	
28	2	S	65	0.0819	97.5	125	140	570	94.411	3.5	36.618	5.55	1.38	42.1	45.5	0.93	

Table (1) – continued.

No.	V_f %	fiber type*	$f_y f_f$	ρ	d (mm)	b (mm)	h (mm)	f_{ct} (MPa)	f'_c (MPa)	ε_o $\times 10^{-3}$	E_c (GPa)	f_{te}^{**} (MPa)	ε_{te}^{***} $\times 10^{-4}$	M_n predicted Eq (5-13) (kN.m)	$M_{n\,exp.}$ (kN.m)	$\frac{M_{n\,pred.}}{M_{n\,exp.}}$	Reference
29	2	S	65	0.0176	101	125	140	490	109.65	4.9	38.432	6.06	1.49	17.3	23.3	0.74	Hannawi et al. [15]
30	2	S	65	0.0324	101.9	125	140	520	109.65	4.9	38.432	6.06	1.49	25.3	31.5	0.80	
31	2	S	65	0	0	100	100	0	104.86	4.4	46.171	5.89	1.45	2.6	3.1	0.90	
32	2	S	65	0	0	100	100	0	94.411	3.5	36.618	5.55	1.38	2.6	2.9	0.90	
33	2	S	65	0	0	100	100	0	109.65	4.9	38.432	6.06	1.49	2.9	3.2	0.91	
34	1.5	S	65	0	0	100	100	0	102.20	4.8	53.265	4.86	1.23	2.8	2.5	0.92	
35	1	S	65	0	0	100	100	0	99.527	4.1	50.379	3.86	1.01	1.9	2.5	1.27	
36	0.5	S	65	0	0	100	100	0	83.109	3.6	42.885	2.38	0.69	1.9	1.9	1.00	
No.	V_f %	fiber type*	$f_y f_f$	ρ	d (mm)	b (mm)	h (mm)	f_{ct} (MPa)	f'_c (MPa)	ε_o $\times 10^{-3}$	E_c (GPa)	f_{te}^{**} (MPa)	ε_{te}^{***} $\times 10^{-4}$	M_n predicted Eq (5-13) (kN.m)	$M_{n\,exp.}$ (kN.m)	$\frac{M_{n\,pred.}}{M_{n\,exp.}}$	Reference
37	2.5	S	65	0	0	100	75	0	151	4.0	44	8.72	2.07	2.3	2.8	0.82	Yoo et al. [13]
38	2.5	S	65	0	0	100	75	0	160	4.0	45	8.69	2.06	2.3	2.5	0.92	
39	2.5	S	65	0	0	100	75	0	149	4.5	43	8.32	1.98	2.2	2.2	1.00	
40	1.25	S	65	0	0	100	75	0	161	4.2	43	6.51	1.59	1.7	1.4	1.21	
41	1.5 S+1 H		65,80	0	0	100	75	0	171	4.0	49	9.06	2.14	2.4	2.5	0.96	
42	2.5	H	80	0	0	100	75	0	157	4.0	40	8.59	2.01	2.3	2.4	0.95	
43	1.0 S+0.5 H		65,80	0	0	100	75	0	169	4.0	46	9.00	2.13	2.2	2.2	1.00	

Table (1) – continued.

No.	V_f %	fiber type*	lf/df	ρ	d (mm)	b (mm)	h (mm)	f_y (MPa)	f'_c (MPa)	ε_o** $\times 10^{-3}$	Ec (GPa)	f_{te}*** (MPa)	ε_{te}**** $\times 10^{-4}$	M_n predicted Eq. (5-18) (kN.m)	$M_{n\ exp.}$ (kN.m)	$\frac{M_{n\ pred.}}{M_{n\ exp.}}$	Reference
44	1	S	65	0	0	40	40	0	166.27	4.21	49.30	6.12	1.5	0.188	0.178	1.06	Yang et al. [6]
45	1.5	S	65	0	0	40	40	0	173.73	4.52	49.83	7.30	1.76	0.223	0.242	0.92	
46	2	S	65	0	0	40	40	0	176.30	4.78	50.23	8.31	1.98	0.252	0.299	0.84	
47	3	S	65	0	0	40	40	0	179.17	5.26	52.37	10.27	2.4	0.309	0.368	0.84	

* (**S**) for straight steel fiber, and (**H**) for hooked steel fiber.
** Calculated by using Eq. (21).
*** Calculated by using Eq. (19).
**** Calculated by using Eq. (22).

REFERENCES

[1] - Gao, R., Stroeven, P., and Hendriks, C. F., "Mechanical Properties of Reactive Powder Concrete Beams", ACI Special Publication, Vol. 228, No. 79, 2005, pp.1237-1252.

[2]- Warnock, R., "Short-Term and Time-Dependent Flexural Behavior of Steel-Fiber Reinforced Reactive Powder Concrete Beams", Ph.D. Thesis, University of New South Wales, 2005, 201 pp.

[3]- Collepardi, S., Coppola, R., Troli, R. and Zaffaroni, P., "Influence of the Superplasticizer Type on the Compressive Strength of Reactive Powder Concrete for Precast Structures", Congress International BIBM, Venzia, 1999, pp. 25-30.

[4]- Dauriac, C. "Special Concrete May Give Steel Stiff Competition", The Seattle Daily Journal of Commerce, May 9, 1997, 5pp.

[5]- Resplendino, J., "State of the Art of Design and Construction of UHPFRC Structures in France", International Symposium on UHPC and Nanotechnology for High Performance Construction Materials, Kassel, March 7-9, 2012.

[6]- Shann, S.V., Harris, D.K., Carbonell, M.A., and Ahlborn, T.M., "Application of Ultra-High Performance Concrete (UHPC) As A Thin-Topped Overlay for Concrete Bridge Decks", International Symposium on UHPC and Nanotechnology for High Performance Construction Materials, Kassel, March 7-9, 2012.

[7]- Sajna, A., Denarie, E., and Bras, V., "Assessment of a UHPFRC Based Bridge Rehabilitation in Slovenia, Two Years after Application", International Symposium on UHPC and Nanotechnology for High Performance Construction Materials, Kassel, March 7-9, 2012.

[8]- Seibert, P., Perry, V., Ghoneim, G., Carson, G., El-Hacha, R., Cariaga, I., and Zakariasen, D., "The First Architectural UHPC Façade Application in North America", International Symposium on UHPC and Nanotechnology for High Performance Construction Materials, Kassel, March 7-9, 2012.

[9]- Acker, P., and Behloul, m., "Ductal® Technology: a Large Spectrum of Properties, a Wide Range of Applications", Proceedings of International Symposium on Ultra High Performance Concrete, University of Kassel, Kassel, Germany, September 13-15, 2004, pp. 11-23.
[10]- RPC Applications, http://www.ductal-lafarge.com/wps/portal/ductal/2-Structural.
[11]- Voo, J., Foster, S., and Gilbert, R., "Shear Strength of Fiber Reinforced Reactive Powder Concrete Girders without Stirrups", the University of New South Wales, Sydney 2052 Australia, UNICIV Report No. R-421 November 2003, 131 pp.
[12]- Yang, I. H., Joh, C., and Kim, B., "Structural Behavior of Ultra High Performance Concrete Beams Subjected to Bending", Engineering Structures, Vol. 32, No. 11, 2010, pp. 3478–3487.
[13]- Al Hassani, H.M., Khalil, W.I., and Danha, L.S., "Mechanical Properties of Reactive Powder Concrete with Various Steel Fiber and Silica Fume Contents", Engineering and Technology Journal, Vol.31, Part (A), No.16, 2013.
[14]- Danha, L.S.," Tensile Behavior of Reactive Powder Concrete", M.Sc. Thesis, University of Technology, Baghdad, 2012.
[15]- Hannawayya, S. PH. Y., "Behavior of Reactive Powder Concrete Beams in Bending", Ph.D. Thesis, University of Technology, Baghdad, 2010.
[16]- Yang, J., Yu, J., Hong, L. and Jian, C., "Mesomechanism of Steel Fiber Reinforcement and Toughening of Reactive Powder Concrete", Science in China Series E-Technological Sciences, Vol. 50, No. 6, 2007, pp. 815-832.
[17]- Al-Hassani, H., M. and Ibraheem, S., K., "A Proposed Equation for the Evaluation of the Nominal Ultimate Bending Moment Capacity of Rectangular Singly Reinforced RPC Sections", Engineering & Technology Journal, Vol. 29, No. 5, 2011.
[18]- ACI 544.4R-88, "Design Consideration for Steel Fiber Reinforced Concrete", American Concrete Institute, Farmington Hills, Michigan, 1999, 18pp.